

# Colloquium Talk

September 2016

Simulation of a  
Double/Triple-Fabry-Pérot-  
Spectropolarimeter  
for the new solar telescope DKIST  
Matthias Johannes Schubert



# Overview

---

The new 4m solar telescope DKIST on Hawaii

Demanded measurement accuracy

The imaging spectropolarimeter:

Visible Tunable Filter VTF

Simulation procedure to model observations with a double/triple *Fabry-Pérot-Interferometer*

Results for simulated observations

Consequences for the instrument configuration

# The new 4m telescope DKIST on Haleakala/Hawaii

Leader ship: National Solar Observatory (US)

**D**aniel K. Inouye **S**olar **T**elescope:

Diameter  $D=4\text{m}$

Photon flux:

$\sim N_{\text{ph}} = 1200$  photons/ms for each resolution element  
in the detector plane (spectral bandwidth  $\Delta\lambda = 6\text{pm}$ )

Spatial resolution:

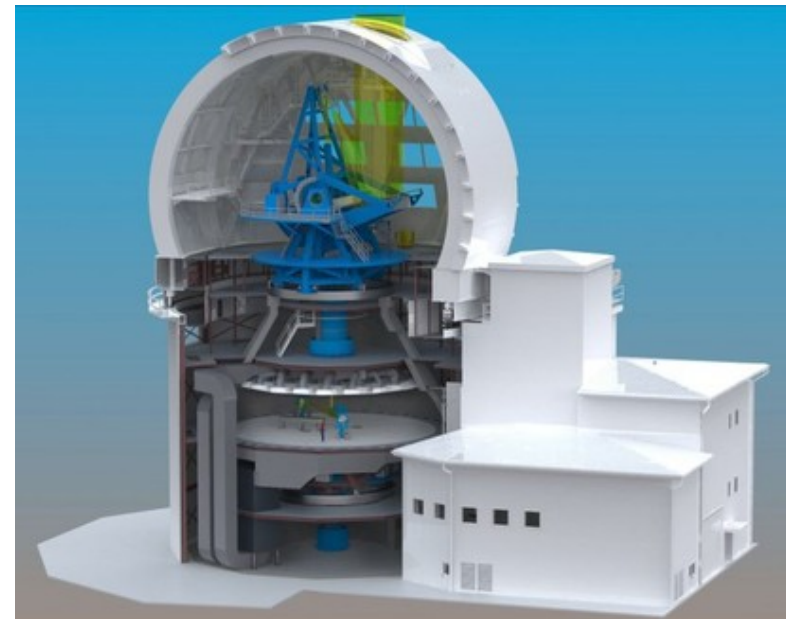
$\Delta\alpha = \lambda/D_T = 0.032'' @ 630.25\text{nm}$

- $\sim 20\text{km}$  for each resolution element in detector plane

## Kiepenheuer-Institut für Sonnenphysik:

Development of an imaging Spectropolarimeter

- Study of solar absorption/emission lines and corresponding magnetic field vectors

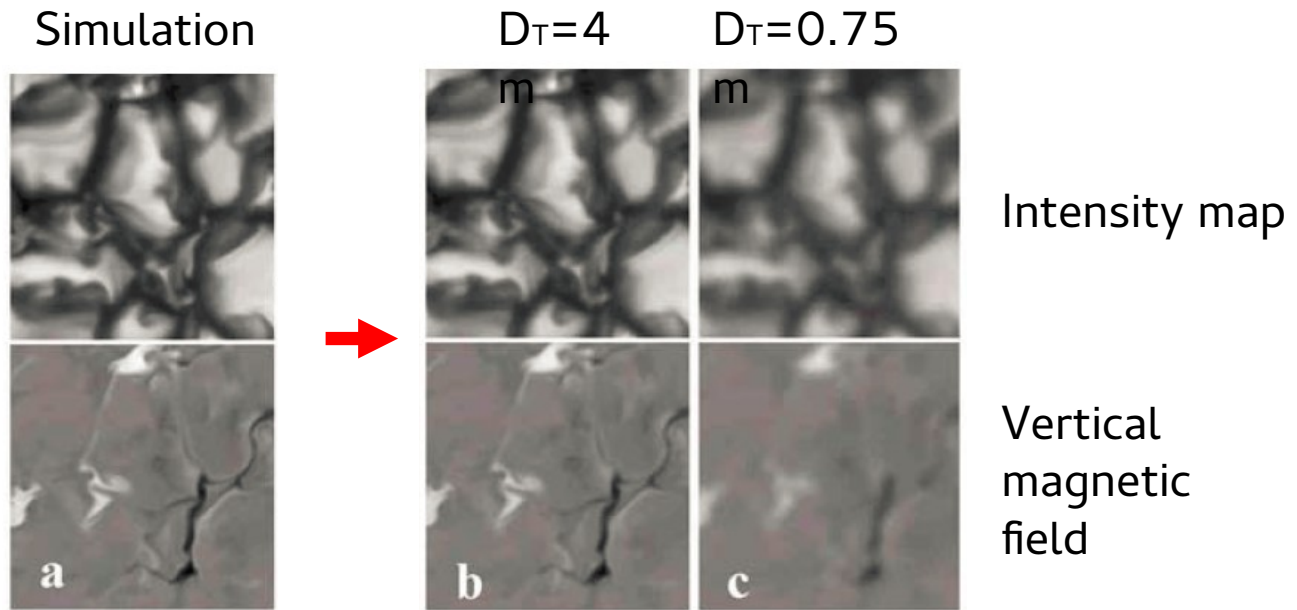


<http://www.kis.uni-freiburg.de/de/projekte/visible-tunable-filter/>

# Required accuracy for physical measurements

**Solar granulation of photosphere**

->  $\lambda_0 = 630.25\text{nm}$ ,  
spatial resolution  
11km



Determination of line core position in the order of 0.2pm

**Accuracy**

Intensity resolution: ~0.2%

**Doppler velocity  $v_D$**

$\Delta v_D = 100\text{ m/s}$

**Full width half maximum**

**W**

**Magnetic field B**

vertical  $B_{\min} = 20\text{G}$

horizontal

$B_{\min} = 100\text{G}$

# 'Visible Tunable Filter' (VTF)

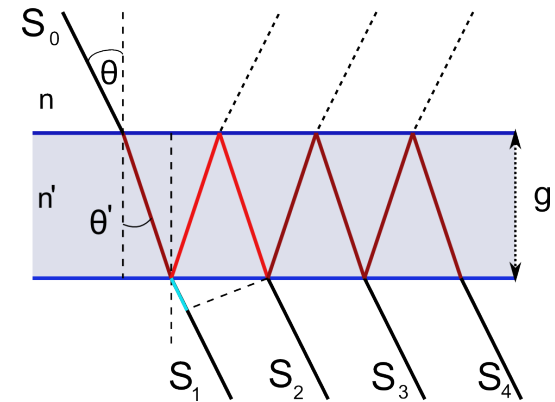


## Configuration of the imaging Spectropolarimeter

- Pre Filter PF - FWHM  $\approx \Delta\lambda = 0.8\text{nm}$
- Polarization modulator  $\mathbf{M} \square (I_{0,1,2,3})$   $T = \mathbf{M}\mathbf{S}$  with Stokes vector  $\mathbf{S} = (I, Q, U, V)^T$

- Multiple Fabry-Pérot-Interferometers FPI

FPI principle: two partly reflecting  
coated glass plates with adjustable  
air gap -> multi beam interference



— Double/Triple system was simulated:

Spectral Resolution  $SR = 100.000/200.000$  (at a central wavelength  $\lambda = 500\text{nm}$ )

— Diameter of active area is  $0.25\text{m} \square$  Field Of View  $FOV = 60^\circ$

— Telecentric mounting

—  $F\# = 200$

Range:  $520\text{-}870\text{ nm}$

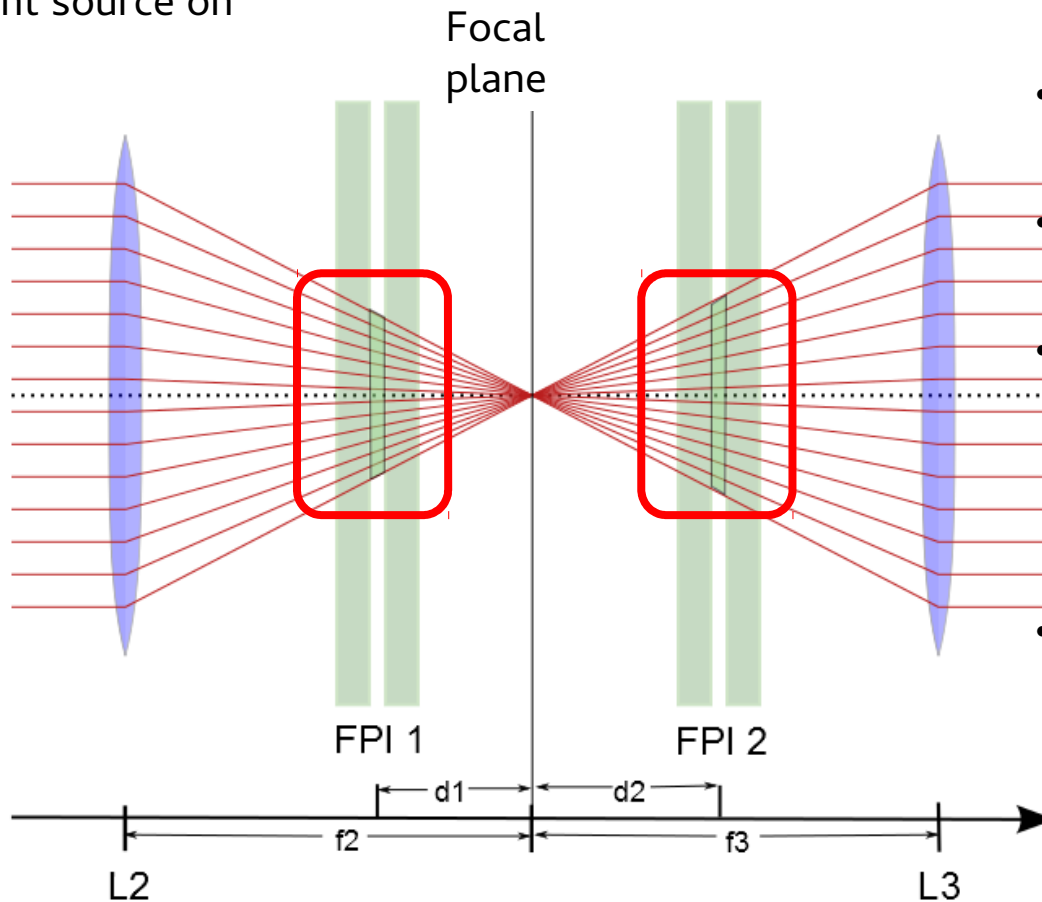


# Double-FPI-system

Induced measurement errors □ variation in the line profile

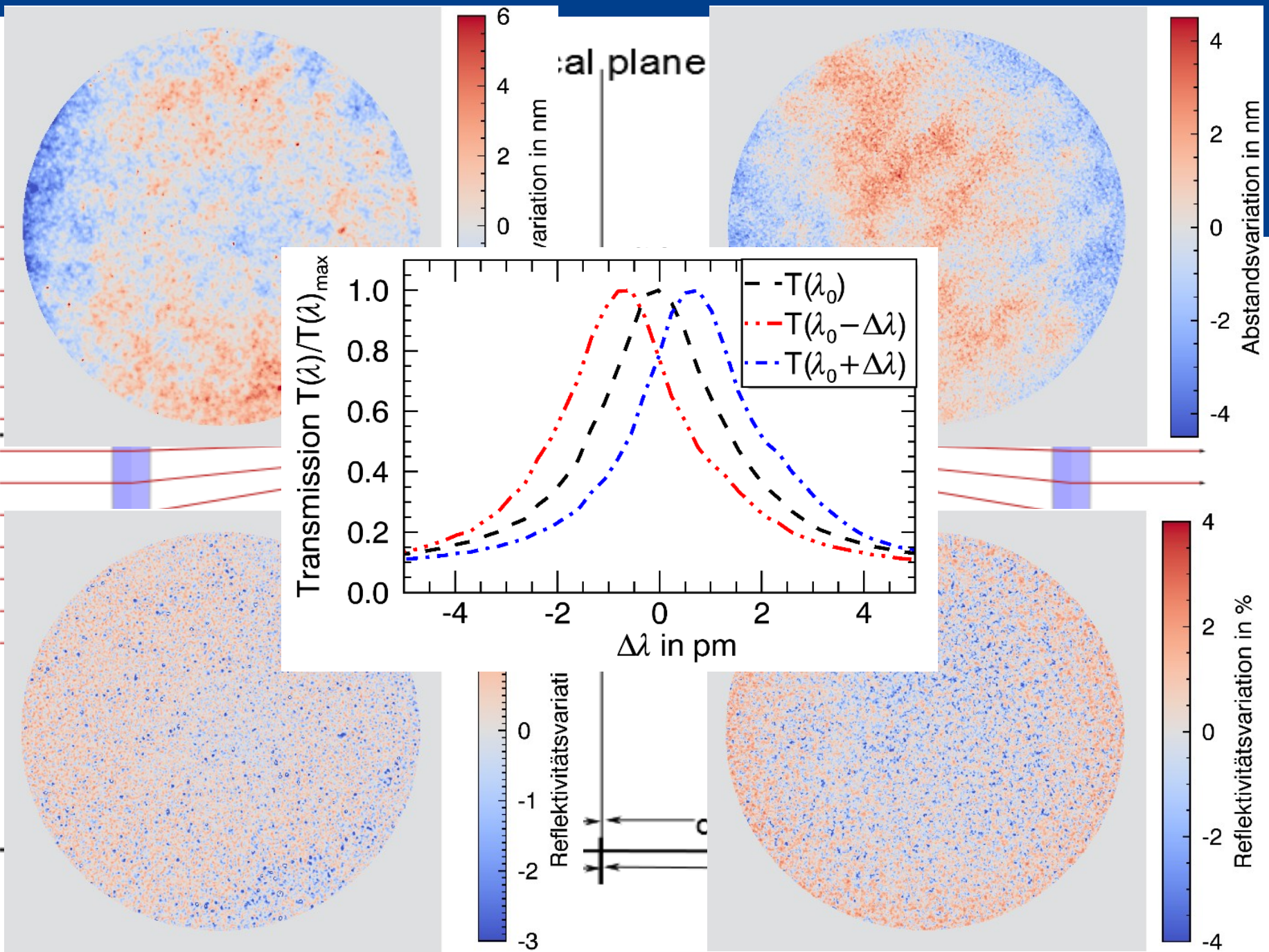
Illustration for a point source on the optical axis

- Light cone is split into individual rays
- each light ray is influenced by a different local plate error



- Gap variation shifts line profile
- Reflectivity error broadens the profile
- Individual shifts of the transmission profiles for FPI1 and FPI2 reduce the photon flux
- Asymmetry due to radial weighting within the integration over the angle spectra

$$I_{x,y}(t) = \sum_{\lambda} I_{x,y,0}(\lambda) \prod_i \sum_{\theta} T_{x,y}^i(\lambda, \theta, R_{x,y}^i, \Delta R_{x,y}^i(\theta), g_{x,y}^i(t), \Delta g_{x,y}^i(\theta))$$





# Combining multiple FPIs

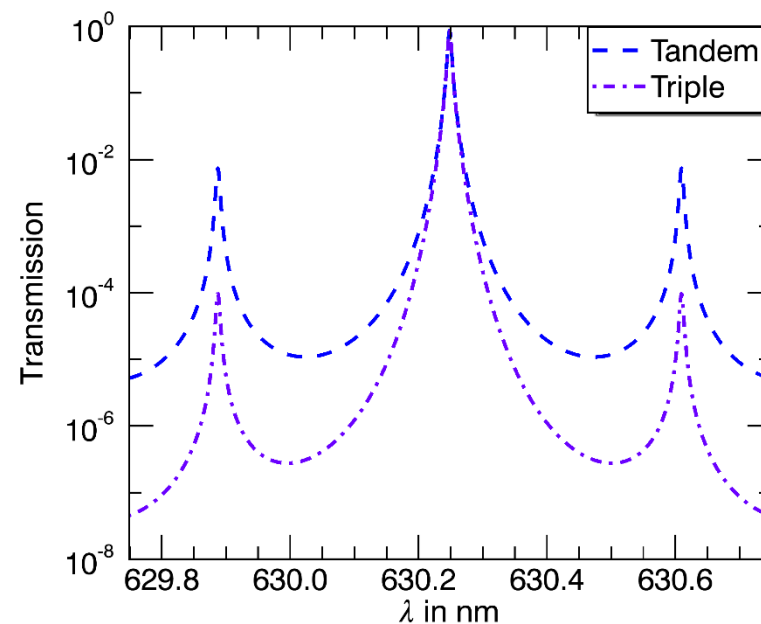
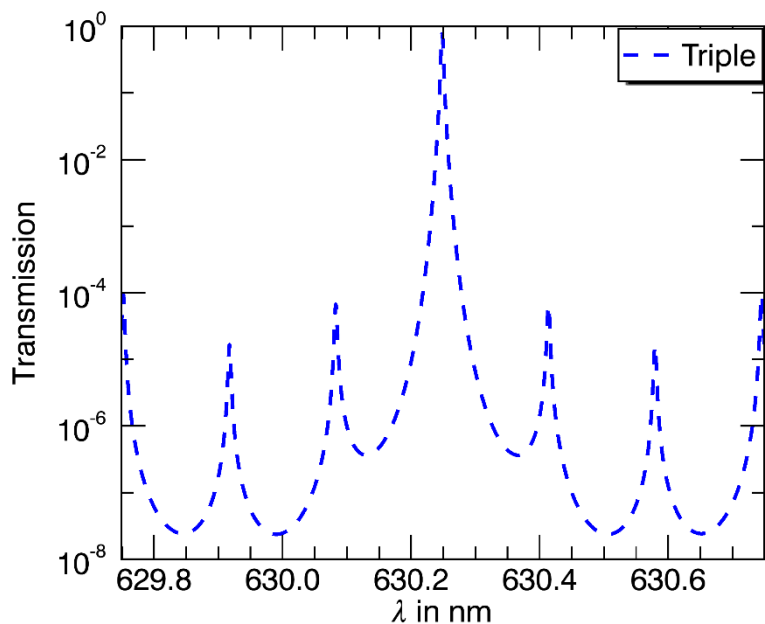
FPI-Parameter for two instrument configurations

Instrument 1

FPI	g in mm	R in %	Finesse $F_i$
1	1.2	94	51
2	0.222	88	25
3	0.352	88	25

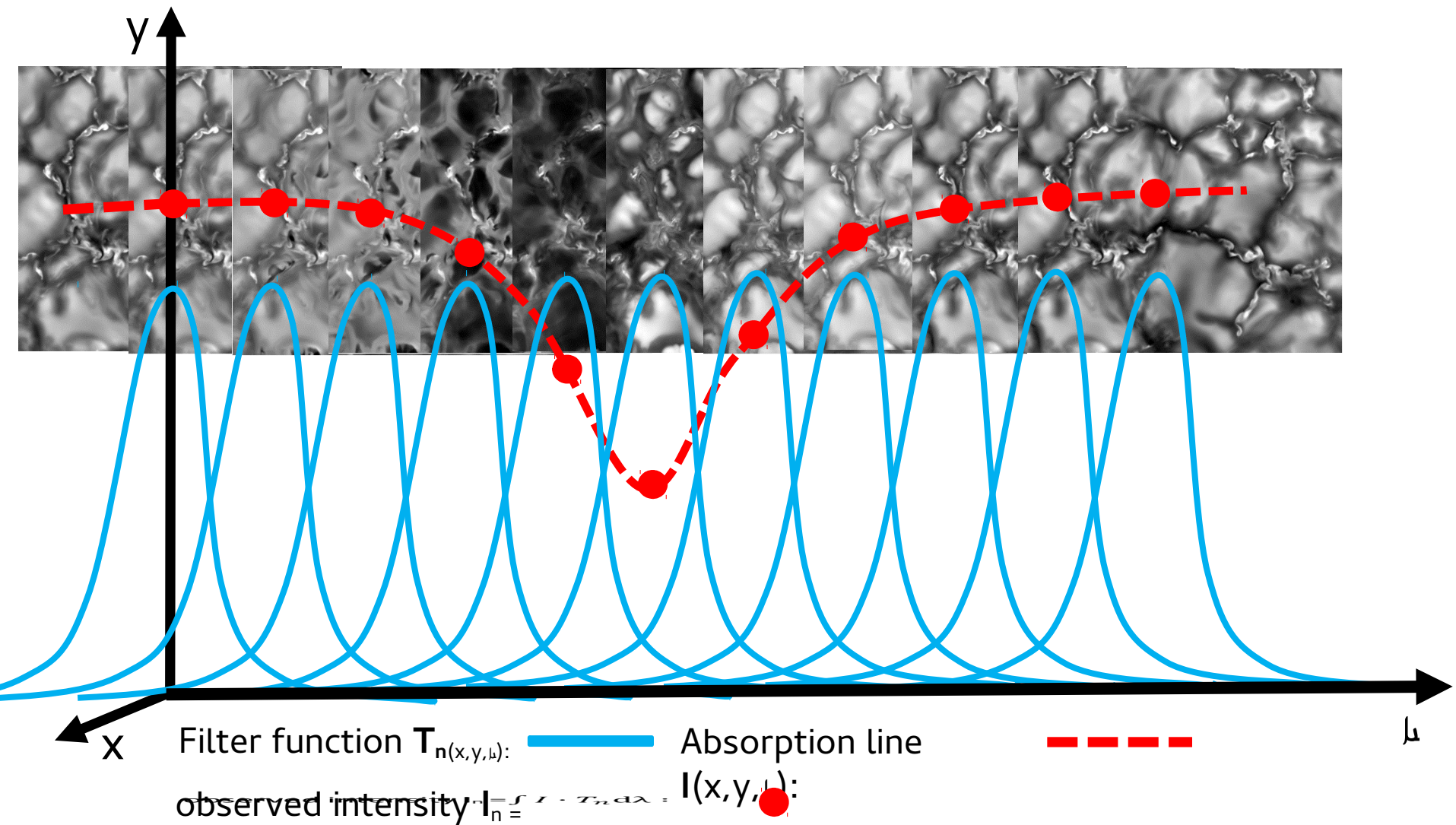
Instrument 2

g in mm	R in %	Finesse $F_i$
0.55	95	61
0.214	84	18
0.149	84	18



# Spectroscopic line scan

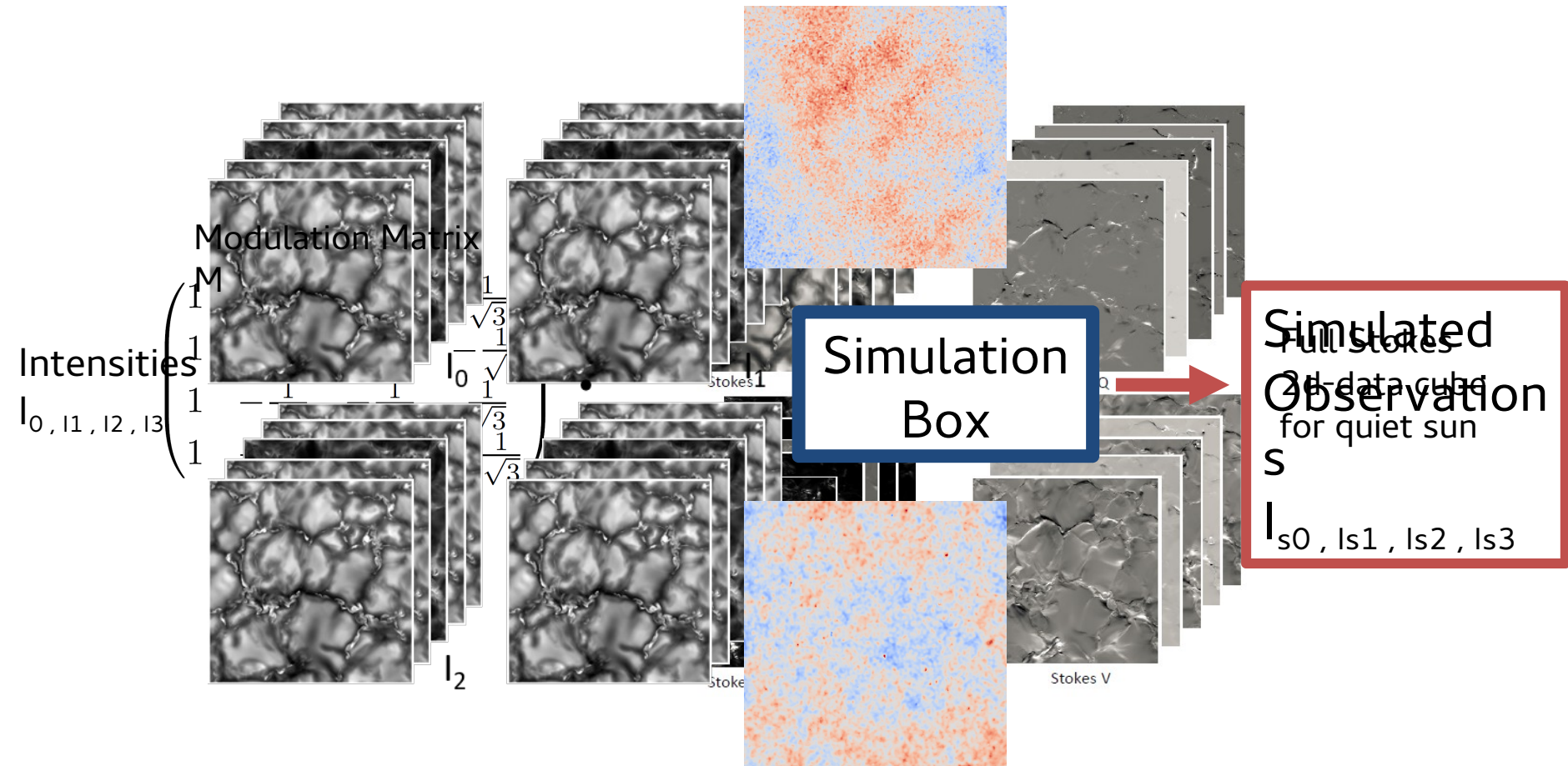
Illustrated for one point in the detector plane



# 2D simulation procedure

Area size on the solar surface: 5000km x 5000km

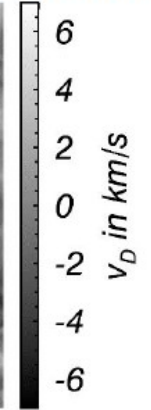
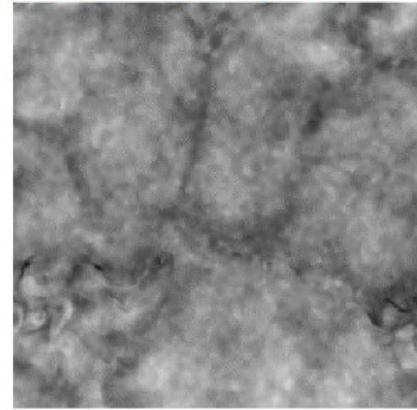
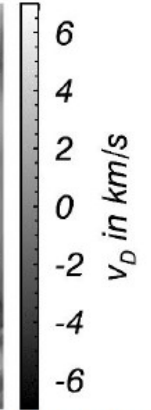
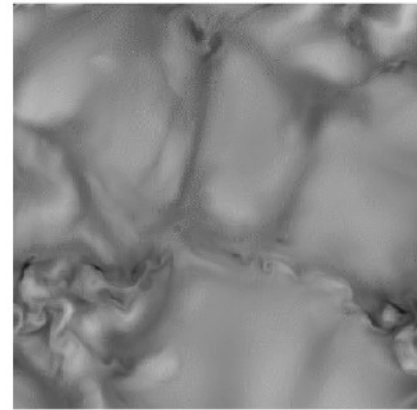
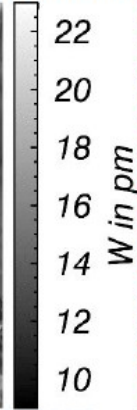
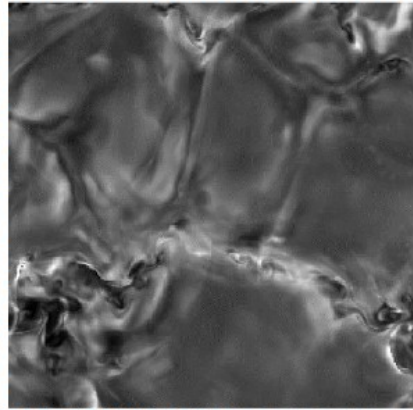
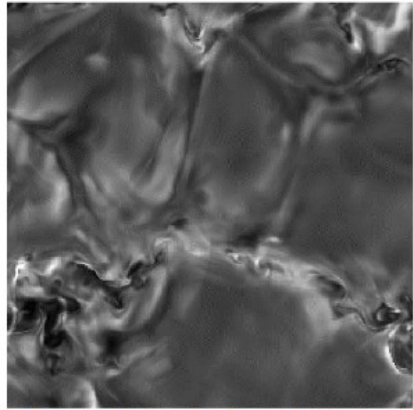
MHD simulations and line synthesis: J. M. Borrero, B. W. Lites, A. Lagg, R. Rezaei, and M. Rempel. Comparison of inversion codes for polarized line formation in MHD simulations. I. Milne-Eddington codes. *Astronomy and Astrophysics*, 572:A54, December 2014



# 2D simulation procedure

Ideale Karten

Intensit  
 $I_{0,11,12,}$

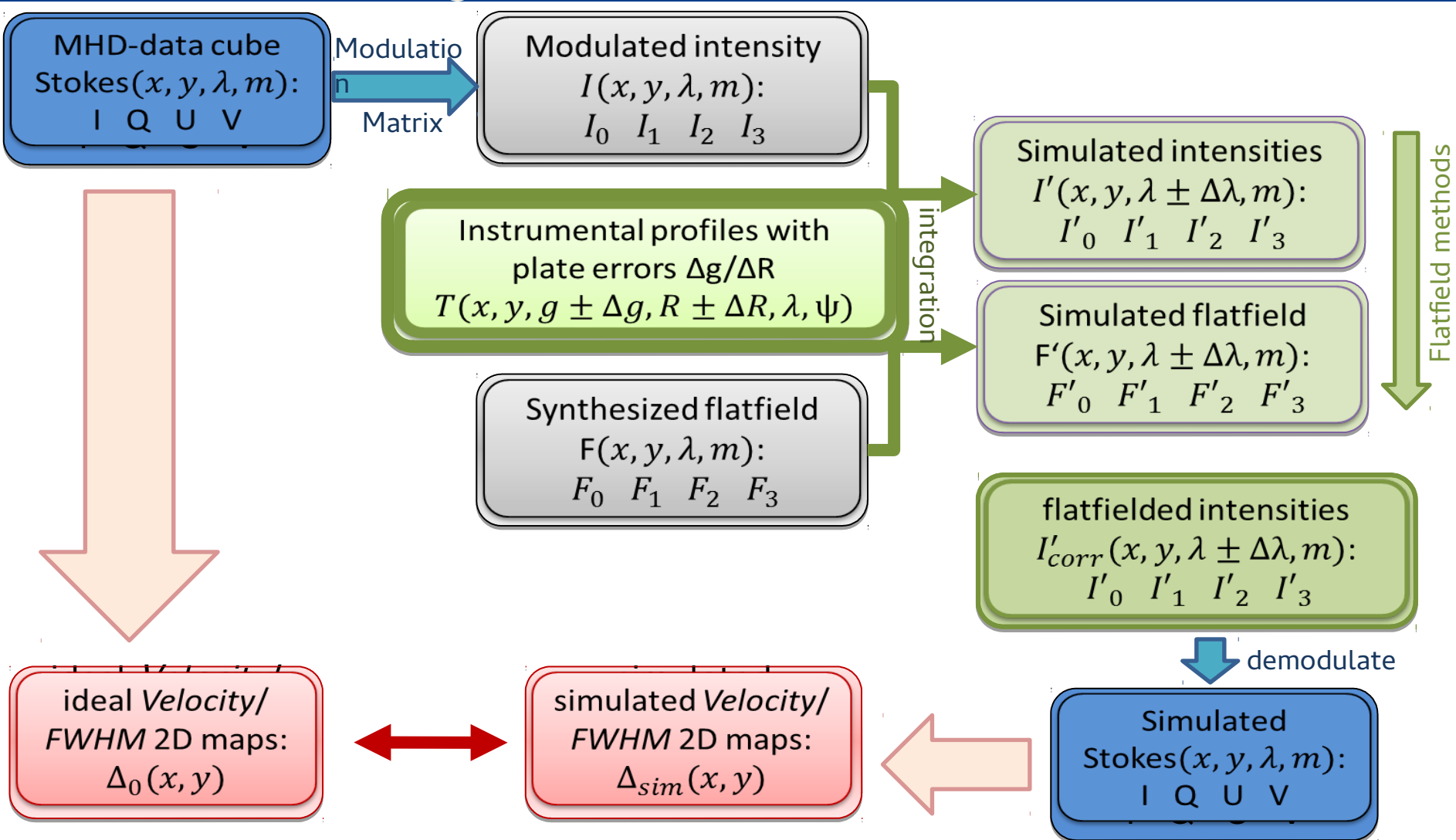


3

3

# 2D Simulations procedure with MESA

## Multi Etalon Simulation Algorithm



# 2D-Simulations – micro roughness

Microroughness: measured with a HeNe laser at VTT/TESOS (testbench) with similar setup

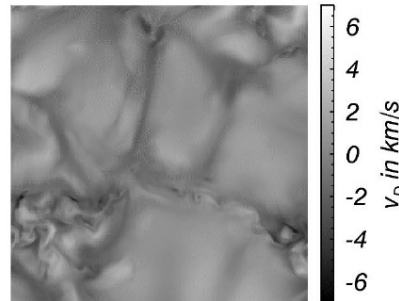
Errors in Doppler velocity, full width half maximum and loss of photon flux for the instruments

FPIs mounted near the focal plane

## Doppler velocity maps

$\lambda_0 = 630.25\text{nm}$  -  $\Delta q_{\text{rms}} = 2.5\text{nm}$

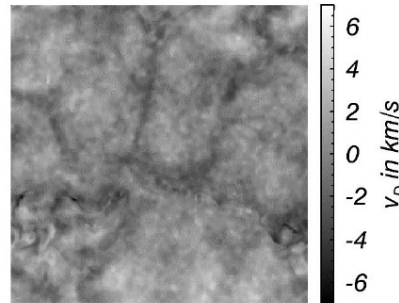
Ideal map



*High resolution mode*

Instrument 1 (Triple)

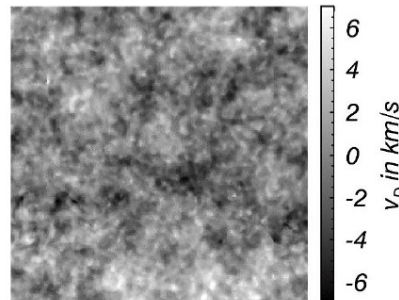
$\lambda_{\mu} = 3.8\text{pm}$



*Fast scan mode*

Instrument 2 (Double)

$\lambda_{\mu} = 6\text{pm}$



## Questions:

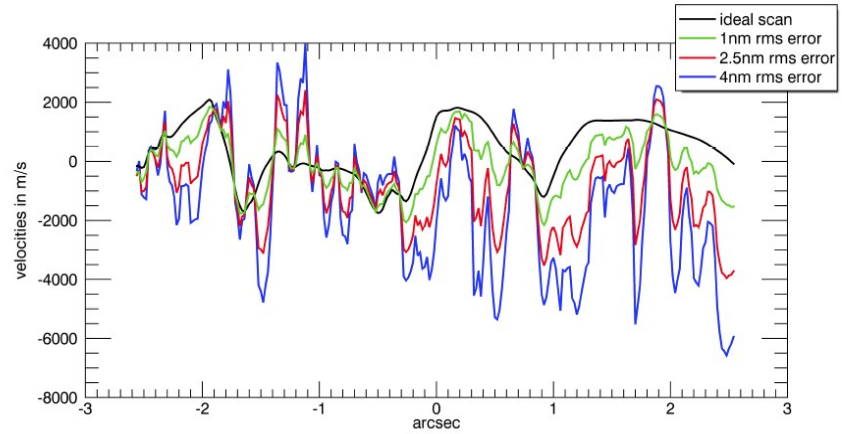
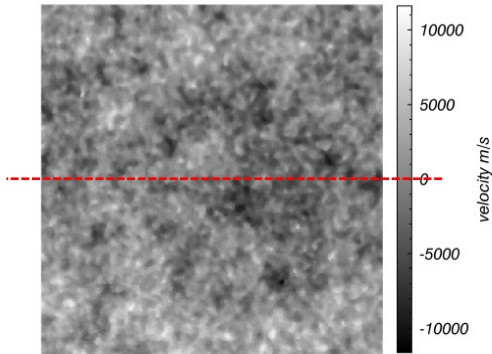
What are the error contributions for a multi-FPI-system with realistic plate error distributions?

Does a defocused mounting of the FPIs in the optical path reduce the errors?

Is it possible to calibrate the induced errors?

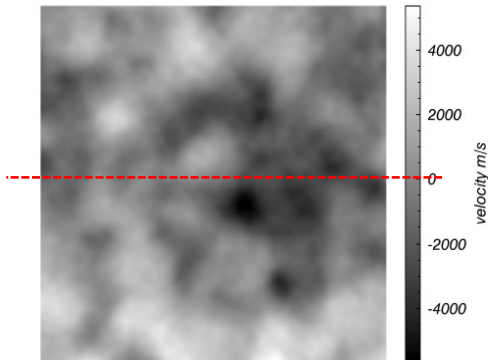
# Illustration of the effect of a defocused mounting

Mounting  
near focal  
plane

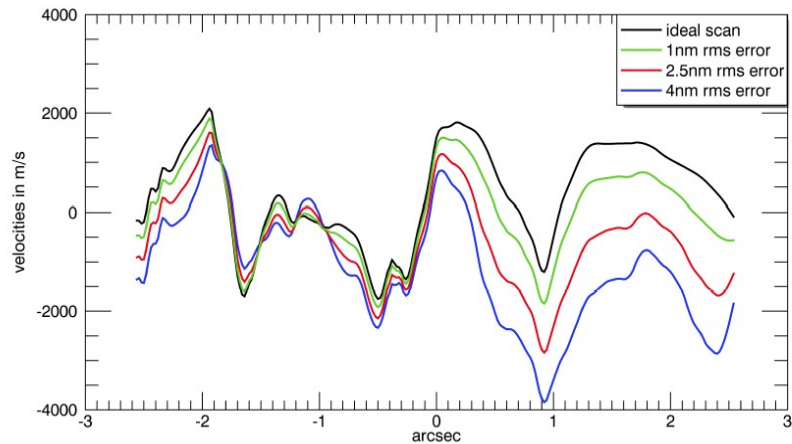


2D Doppler  
maps

Defocused  
mounting



Resulting velocities for a micro  
roughness:

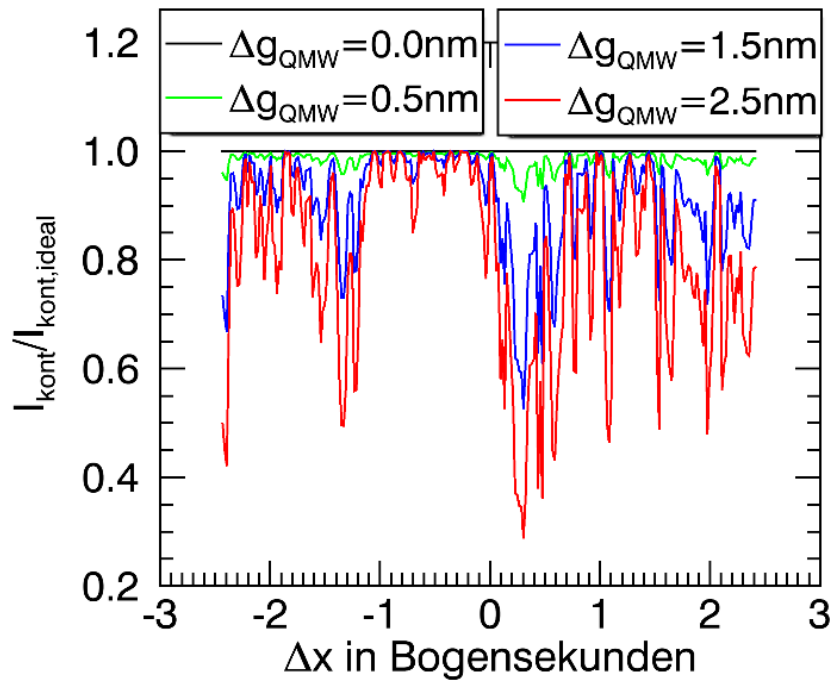


# Simulated observations for different mountings of the FPI

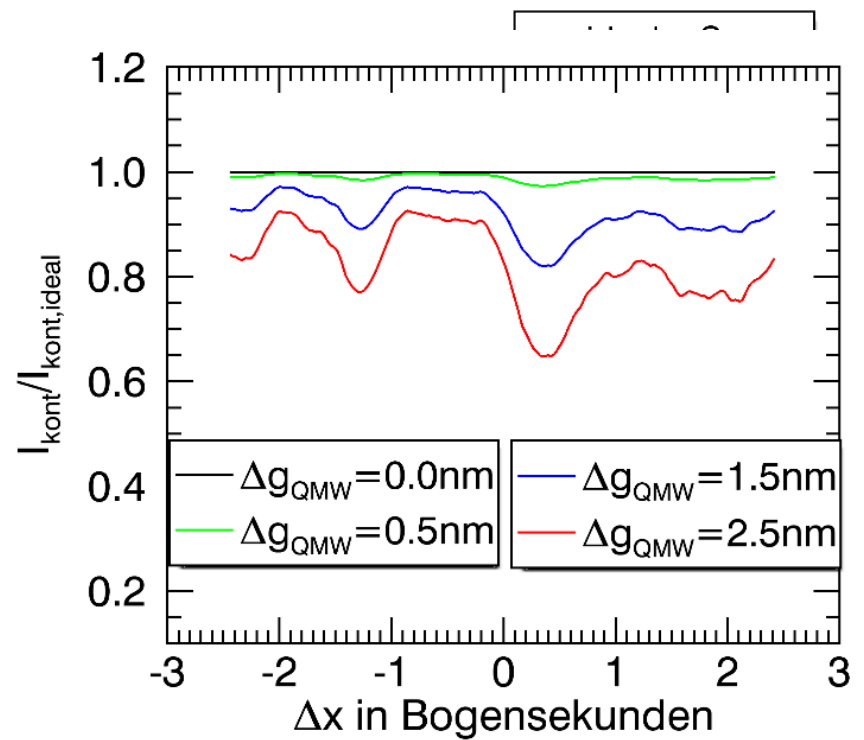
Slices through the middle for a simulated FOV of 5" are shown for Instrument 2

- spectral resolution 100.000@500nm -

Near focal plane



Defocused mounting



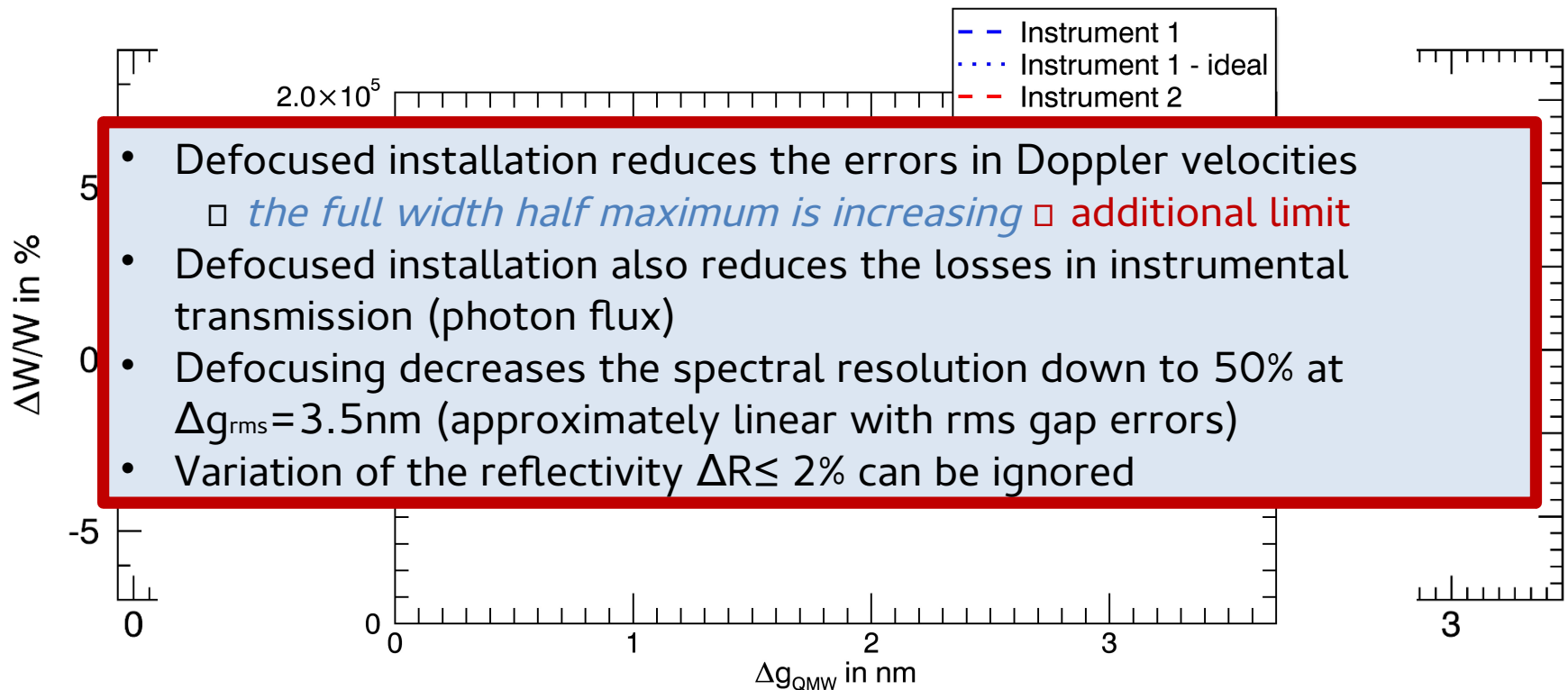


# Results for micro roughness

Shown are the rms values for the simulated field of view

near focal plane

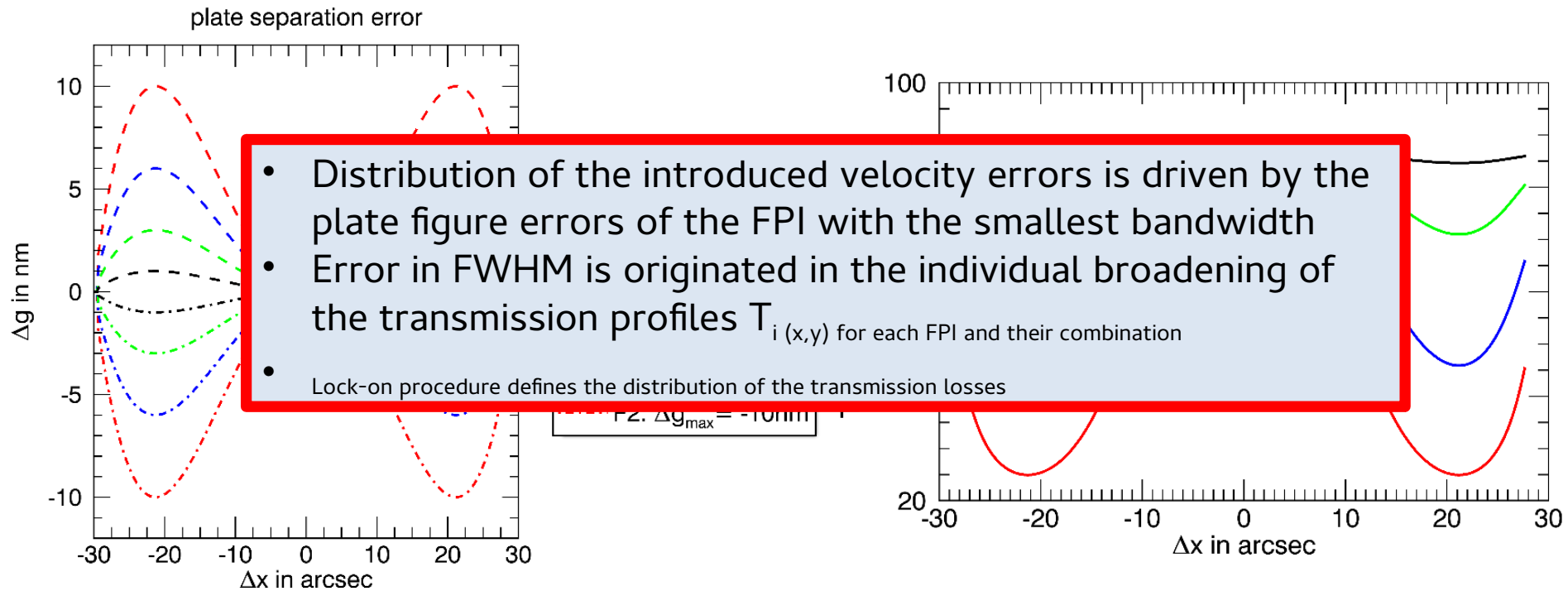
defocuse



# Transmission losses for plate figure errors

For one resolution element, the error stays constant  $\rightarrow \Delta g(\theta)|_{x,y} = \Delta g|_{x,y}$  and  $\Delta R(\theta)|_{x,y} = \Delta R|_{x,y}$

Shown are the total instrument transmissions  $T$  for a slice through the middle of a simulated FOV=60''



# Results for simulated plate gap errors

	FPI mounting	$\Delta v_{D,rms} / \text{nm}$	$\Delta v_D / \text{nm}$	$\Delta W_{rms} / \text{nm}$	$\Delta W / \text{nm}$																																				
Instrument 1	focus	335 m/s	36 m/s	1.0 %	1.6 %																																				
	defocus	235 m/s	54 m/s	<table border="1"> <thead> <tr> <th></th> <th>FPI mounting</th> <th><math>\Delta v_{D,rms} / \text{nm}</math></th> <th><math>\sigma_{v_D} / \text{nm}</math></th> <th><math>\Delta W_{rms} / \text{nm}</math></th> <th><math>\sigma_{\Delta W} / \text{nm}</math></th> </tr> </thead> <tbody> <tr> <td>Instrument 1</td> <td>focus</td> <td>335 m/s</td> <td>36 m/s</td> <td>1.0 %</td> <td>1.6 %</td> </tr> <tr> <td></td> <td>defocus</td> <td>235 m/s</td> <td>54 m/s</td> <td><math>0.2\% \cdot \Delta g + 0.8\% \cdot \Delta g^2</math></td> <td>1.0%</td> </tr> <tr> <td>Instrument 2</td> <td>focus</td> <td>685 m/s</td> <td>50 m/s</td> <td>0.8 %</td> <td>2.0 %</td> </tr> <tr> <td></td> <td>defocus</td> <td>457 m/s</td> <td>14 m/s</td> <td><math>1.8\% \cdot \Delta g + 1.2\% \cdot \Delta g^2</math></td> <td>1.0%</td> </tr> <tr> <td></td> <td>defocus, figure</td> <td>564 m/s</td> <td>43 m/s</td> <td>0.3 %</td> <td>1.9 %</td> </tr> </tbody> </table>		FPI mounting	$\Delta v_{D,rms} / \text{nm}$	$\sigma_{v_D} / \text{nm}$	$\Delta W_{rms} / \text{nm}$	$\sigma_{\Delta W} / \text{nm}$	Instrument 1	focus	335 m/s	36 m/s	1.0 %	1.6 %		defocus	235 m/s	54 m/s	$0.2\% \cdot \Delta g + 0.8\% \cdot \Delta g^2$	1.0%	Instrument 2	focus	685 m/s	50 m/s	0.8 %	2.0 %		defocus	457 m/s	14 m/s	$1.8\% \cdot \Delta g + 1.2\% \cdot \Delta g^2$	1.0%		defocus, figure	564 m/s	43 m/s	0.3 %	1.9 %	1.0%
	FPI mounting	$\Delta v_{D,rms} / \text{nm}$	$\sigma_{v_D} / \text{nm}$	$\Delta W_{rms} / \text{nm}$	$\sigma_{\Delta W} / \text{nm}$																																				
Instrument 1	focus	335 m/s	36 m/s	1.0 %	1.6 %																																				
	defocus	235 m/s	54 m/s	$0.2\% \cdot \Delta g + 0.8\% \cdot \Delta g^2$	1.0%																																				
Instrument 2	focus	685 m/s	50 m/s	0.8 %	2.0 %																																				
	defocus	457 m/s	14 m/s	$1.8\% \cdot \Delta g + 1.2\% \cdot \Delta g^2$	1.0%																																				
	defocus, figure	564 m/s	43 m/s	0.3 %	1.9 %																																				
Instrument 2	focus	685 m/s	50 m/s	0.8 %	2.0 %																																				
	defocus	457 m/s	14 m/s	<table border="1"> <thead> <tr> <th></th> <th>FPI mounting</th> <th><math>\Delta v_{D,rms} / \text{nm}</math></th> <th><math>\sigma_{v_D} / \text{nm}</math></th> <th><math>\Delta W_{rms} / \text{nm}</math></th> <th><math>\sigma_{\Delta W} / \text{nm}</math></th> </tr> </thead> <tbody> <tr> <td>Instrument 1</td> <td>focus</td> <td>335 m/s</td> <td>36 m/s</td> <td>1.0 %</td> <td>1.6 %</td> </tr> <tr> <td></td> <td>defocus</td> <td>235 m/s</td> <td>54 m/s</td> <td><math>0.2\% \cdot \Delta g + 0.8\% \cdot \Delta g^2</math></td> <td>1.0%</td> </tr> <tr> <td>Instrument 2</td> <td>focus</td> <td>685 m/s</td> <td>50 m/s</td> <td>0.8 %</td> <td>2.0 %</td> </tr> <tr> <td></td> <td>defocus</td> <td>457 m/s</td> <td>14 m/s</td> <td><math>1.8\% \cdot \Delta g + 1.2\% \cdot \Delta g^2</math></td> <td>1.0%</td> </tr> <tr> <td></td> <td>defocus, figure</td> <td>564 m/s</td> <td>43 m/s</td> <td>0.3 %</td> <td>1.9 %</td> </tr> </tbody> </table>		FPI mounting	$\Delta v_{D,rms} / \text{nm}$	$\sigma_{v_D} / \text{nm}$	$\Delta W_{rms} / \text{nm}$	$\sigma_{\Delta W} / \text{nm}$	Instrument 1	focus	335 m/s	36 m/s	1.0 %	1.6 %		defocus	235 m/s	54 m/s	$0.2\% \cdot \Delta g + 0.8\% \cdot \Delta g^2$	1.0%	Instrument 2	focus	685 m/s	50 m/s	0.8 %	2.0 %		defocus	457 m/s	14 m/s	$1.8\% \cdot \Delta g + 1.2\% \cdot \Delta g^2$	1.0%		defocus, figure	564 m/s	43 m/s	0.3 %	1.9 %	1.0%
	FPI mounting	$\Delta v_{D,rms} / \text{nm}$	$\sigma_{v_D} / \text{nm}$	$\Delta W_{rms} / \text{nm}$	$\sigma_{\Delta W} / \text{nm}$																																				
Instrument 1	focus	335 m/s	36 m/s	1.0 %	1.6 %																																				
	defocus	235 m/s	54 m/s	$0.2\% \cdot \Delta g + 0.8\% \cdot \Delta g^2$	1.0%																																				
Instrument 2	focus	685 m/s	50 m/s	0.8 %	2.0 %																																				
	defocus	457 m/s	14 m/s	$1.8\% \cdot \Delta g + 1.2\% \cdot \Delta g^2$	1.0%																																				
	defocus, figure	564 m/s	43 m/s	0.3 %	1.9 %																																				
	defocus, figure	564 m/s	43 m/s	0.3 %	1.9 %																																				

# Magnetic sensitivity – 1D Simulation

- Photon noise  $n = \sqrt{N_{ph}}$ 
  - transmission of the instrument, telescope and all the optical parts (telescope, coude table and polarizing beamsplitter  $t=0.7$ )
  - efficiency of the detector  $\epsilon=0.56$
  - exposure time  $t=225$ ms

→ Instrument 1:  $SNR = N_{ph} / n = 560$

→ Instrument 2:  $SNR=710$

□ Instrument 2:  $SNR=710$

- Inversion code **SIR** for line synthesis and inversion

- B. Ruiz Cobo and J. C. del Toro Iniesta. Inversion of Stokes profiles. The Inversion code **SIR** for line synthesis and inversion  
Astrophysical Journal, 398:375–385, October 1992. doi: 10.1086/171862

B. Ruiz Cobo and J. C. del Toro Iniesta. Inversion of Stokes profiles. The Astrophysical Journal, 398:375–385, October 1992. doi: 10.1086/171862

– atmosphere model: HSRA

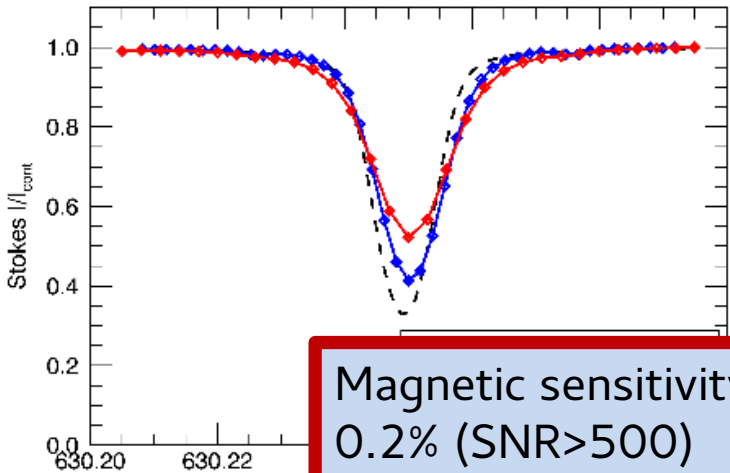
– Fe I 630.25nm: line synthesis for different magnetic field strengths and inclinations  
atmosphere model: HSRA

– Fe I 630.25nm: line synthesis for different magnetic field strengths and inclinations

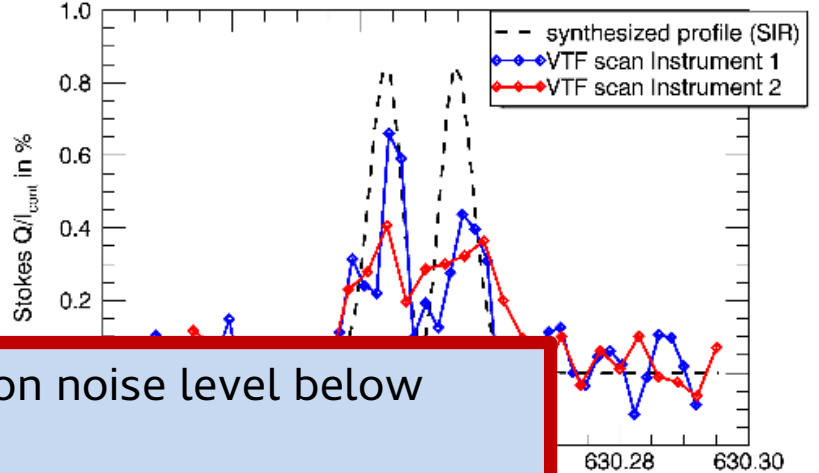
# Simulations for a horizontal magnetic field vector

Full Stokes vector I, Q, U and V is shown

160G, horizontal field: Stokes I synthesized (SIR) vs simulated scan VTF



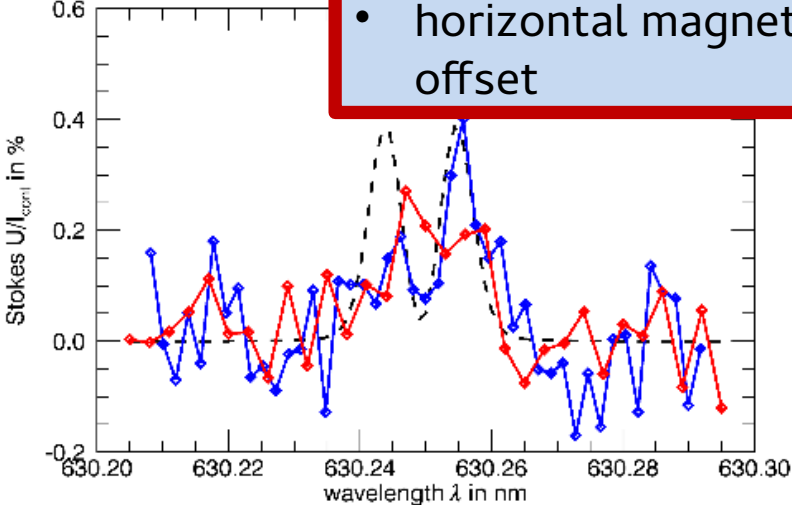
160G, horizontal field: Stokes Q synthesized (SIR) vs simulated scan VTF



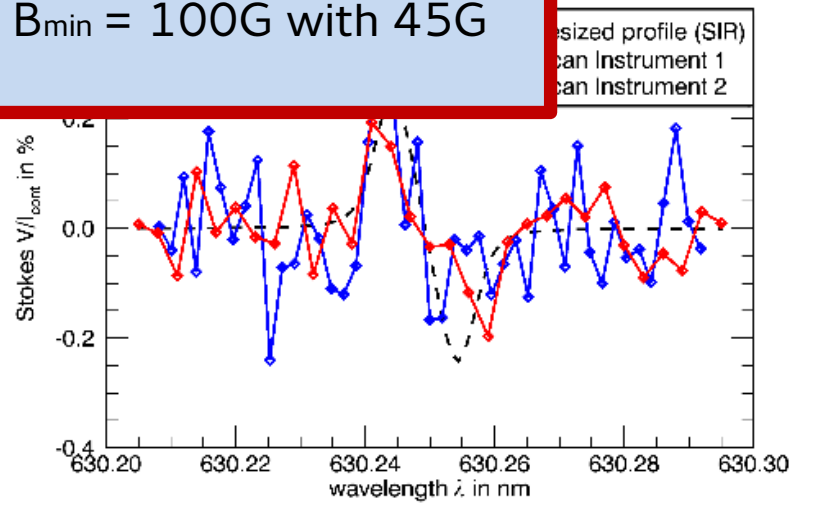
Magnetic sensitivity for photon noise level below 0.2% (SNR>500)

- vertical magnetic fields:  $B_{min} = 20G$
- horizontal magnetic fields:  $B_{min} = 100G$  with 45G offset

160G, horizontal field: Stokes U synthesized (SIR) vs simulated scan VTF



160G, horizontal field: Stokes V synthesized (SIR) vs simulated scan VTF

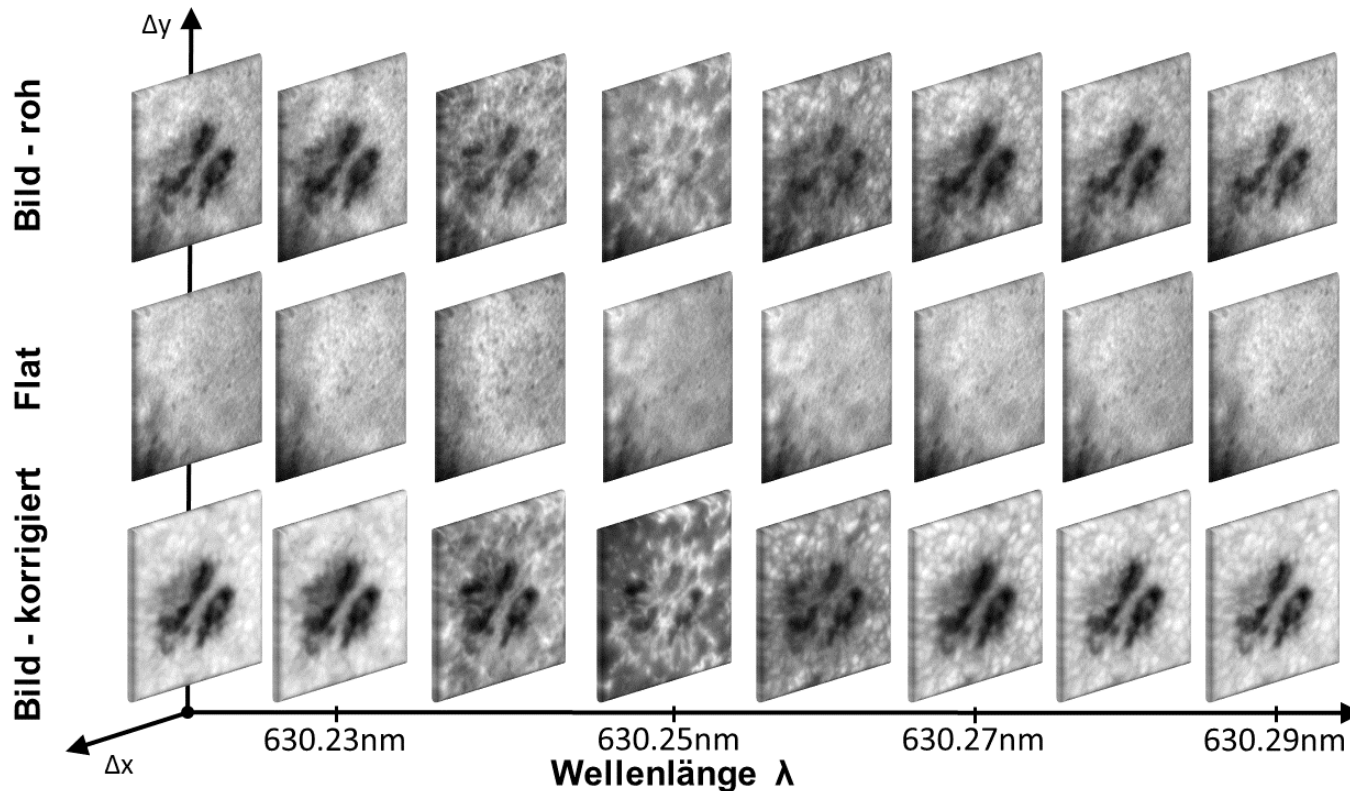


# Data calibration

Enhancement of the standard procedure – shown for instrument 2 in Tandem configuration in a defocused mounting of the FPI on the optical axis

## Standard method for 2d image calibration

- The error in the contrast is corrected very well



Problem for solar spectroscopic observations: calibrating the data will introduce additional errors in terms of shifting the line profile and broadening the FWHM in an uncontrolled way

# Flatfield methods

Three flatfield approaches and their differences

$$\text{Gain}_0(x, y, \lambda) = \frac{[\text{Flat}(x, y, \lambda) - \text{Dark}(x, y)]}{\langle [\text{Flat}(x, y, \lambda) - \text{Dark}(x, y)] \rangle}$$

*Calculate the gain table*

$$\text{Gain}_1(x, y, \lambda) = \frac{[\text{Flat}(x, y, \lambda) - \text{Dark}(x, y)]}{\langle [\text{Flat}(x, y, \lambda) - \text{Dark}(x, y)] |_{\pm \Delta \lambda(x, y)} \rangle}$$

$$\text{Gain}_2(x, y, \lambda) = \frac{[\text{Flat}(x, y, \lambda) - \text{Dark}(x, y)]}{\langle [\text{Flat}(x, y, \lambda \pm \Delta \lambda(x, y)) - \text{Dark}(x, y)] \rangle}$$

*Correct the data*

$$I'(x, y, \lambda) = \frac{[I_0(x, y, \lambda) - \text{Dark}(x, y)]}{\text{Gain}(x, y, \lambda)}$$

Determined 2D map of introduced shifts in line core position  $\lambda_0$

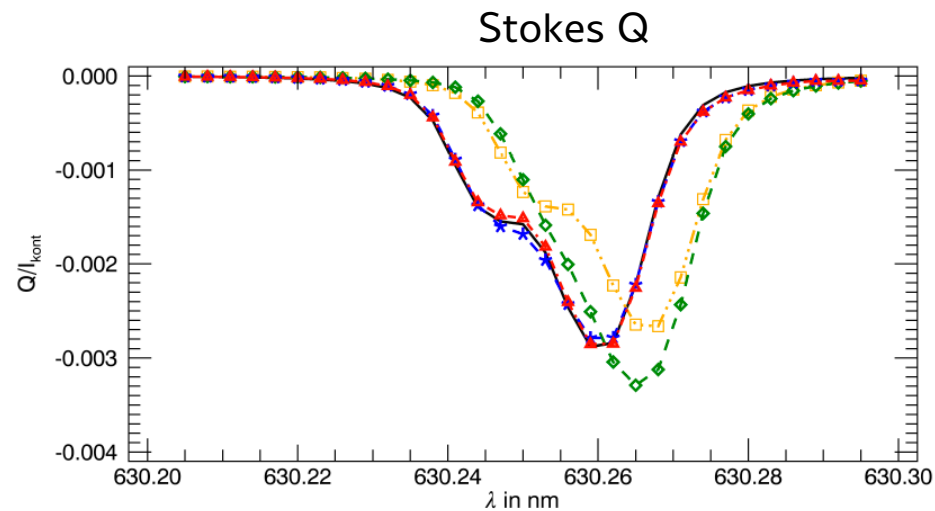
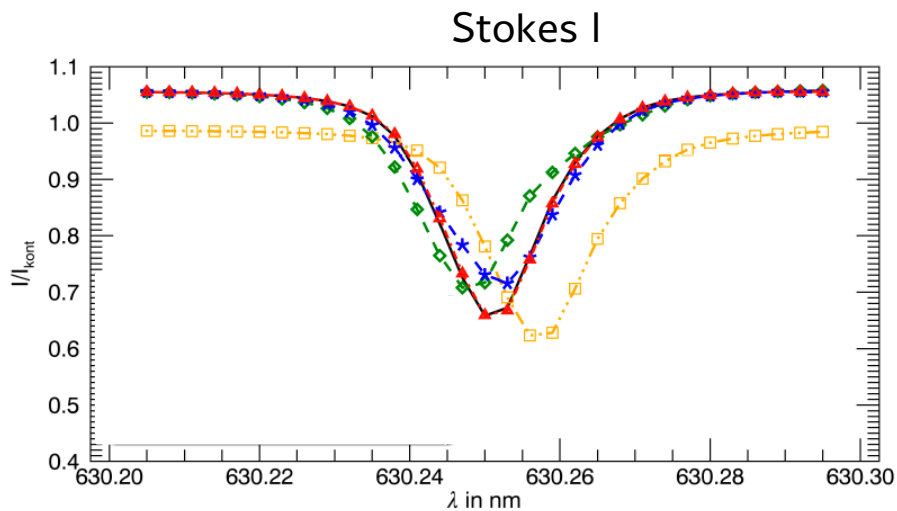
*Calculate i.e. the Doppler velocity maps  $v_{D(x,y)}$*

$$\Delta \lambda_D(x, y) = \Delta \lambda'_D(x, y) \pm \Delta \lambda(x, y)$$

$$v_D(x, y) = \frac{\Delta \lambda_D(x, y)}{\lambda_0} \cdot c$$

# Differences in calibration methods

The calibration methods are illustrated for a full Stokes vector I, Q, U and V with a plate gap error  $\Delta g_{\text{rms}}=3\text{nm}$



\*\*\* Simulated observations

\*\*\* Calibration method

2

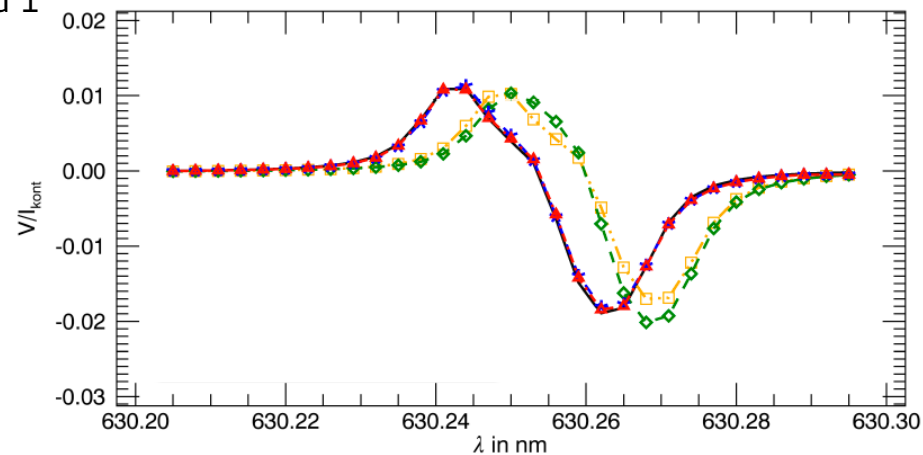
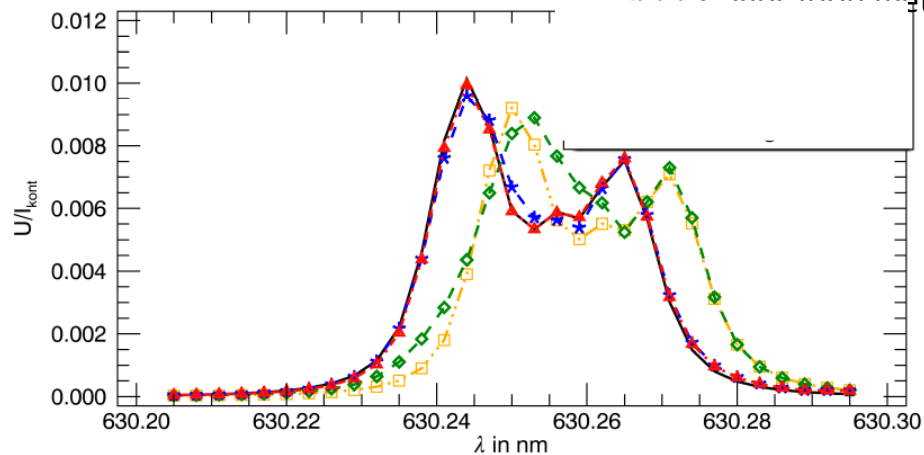
Stokes U

\*\*\* Standard data calibration

\*\*\* Calibration method 1

--- Ideal

### Stokes V



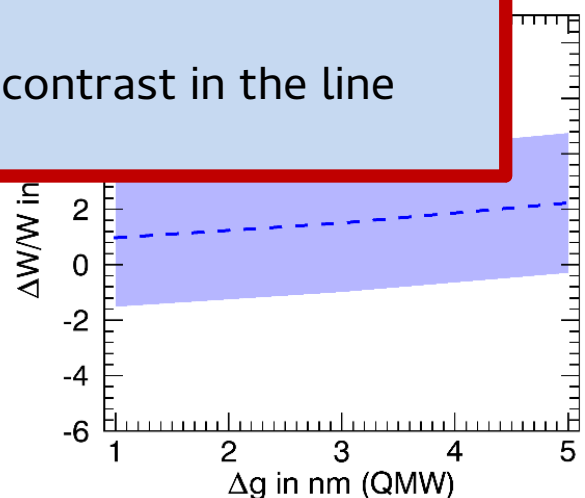
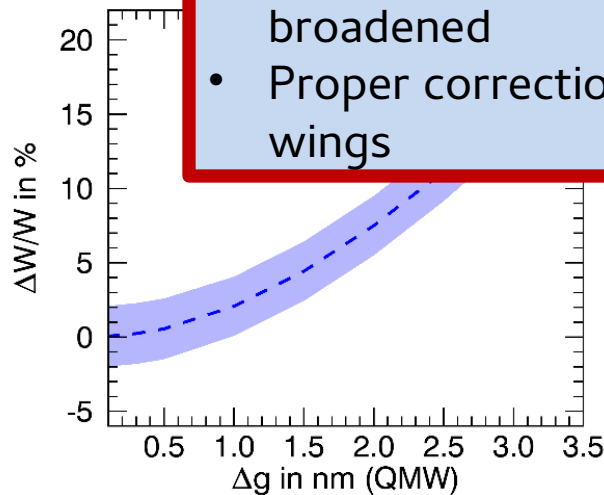
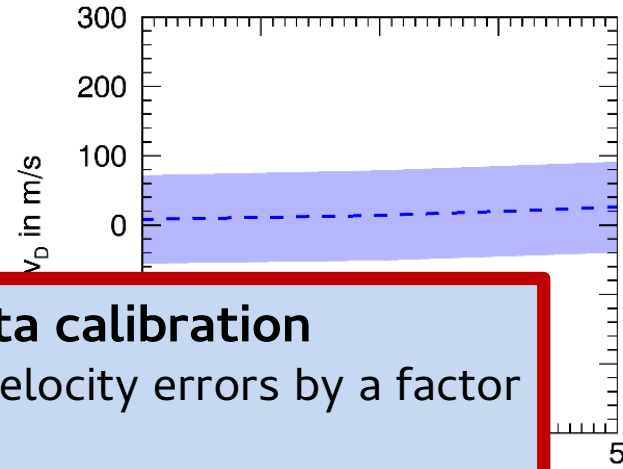
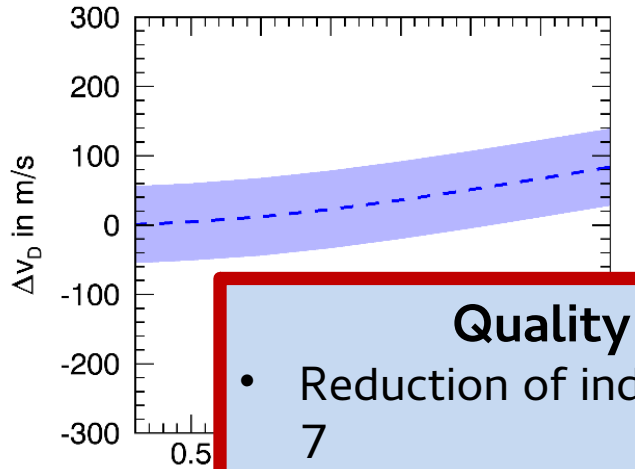


# Data calibration and the benefit on physical measurements

## - Calibration method 2 -

Micro roughness

Plate figure errors



### Quality of data calibration

- Reduction of induced velocity errors by a factor 7
- FWHM of absorption profiles is not additionally broadened
- Proper correction of the contrast in the line wings

# Consequences for the VTF

Instrument 1 or Instrument 2

**We will realize instrument 2 in tandem configuration for the VTF:**

Defined values for the manufacturing process to achieve the demanded measurement accuracy

- Minor losses in the photo individual transmission process element
- The higher induced velocity well with the shown data

- Demanded magnetic sensitivity velocity measurements and the FWHM is fulfilled
- Shorter cadence for line acquisition due to lower spectral resolution

Error distribution	Surface error $\Delta r$ (rms) Reflectivity error $\Delta R$ (rms)
Micro roughness	$\Delta r \leq 0.5\text{nm}$ $\Delta R \leq 2\%$
Plate figure errors	$\Delta r \leq 5\text{nm}$ $\Delta R \leq 2\%$

Thank you for your kind  
attention!

Questions?